

TOWARD A BETTER UNDERSTANDING OF DESILICATION PRODUCT (DSP) PRECIPITATION KINETICS

LaMacchia, R.

Technology Delivery Group, Alcoa World Alumina, Western Australia, Australia

Abstract

Deriving kinetics equations for DSP precipitation can be difficult because of the simultaneous effects of two concurrent processes, namely reactive silica dissolution and DSP precipitation. In this work, a more fundamental approach has been sought, to further understand DSP precipitation mechanisms over wide ranging sets of conditions. While the literature has historically reported growth rates for this reaction, DSP growth is not the sole mechanism at play. For this reason, conventional methods for obtaining the kinetic rate constant and order are confounded. In modelling the pre-digestion circuit of an alumina refinery, it is hypothesized that secondary nucleation is the dominant mechanism, allowing a conventional fit to an empirical kinetic equation with order, $n = 1.81 \pm 0.63$.

1. Introduction

The problem of obtaining a kinetic DSP precipitation equation is by no means a new one, with many authors having attempted to realise values for the unknowns in variants of the following kinetic desupersaturation equation:

$$-d\sigma/dt = k.A.\sigma^n$$

Where: σ is the relative supersaturation ratio, $\sigma = ([\text{SiO}_2] - [\text{SiO}_2]^*) / [\text{SiO}_2]^*$

$[\text{SiO}_2]^*$ is the silica solubility concentration

A is the area of seed material per unit volume, in $\text{m}^2.\text{L}^{-1}$

$k = k_0.e^{(-E_a/RT)}$ is the pre-exponential factor multiplied by the Arrhenius term, in $\text{L}.\text{m}^{-2}.\text{h}^{-1}$

E_a is the activation energy, in $\text{J}.\text{mol}^{-1}$

t is time, in h

R is the universal gas constant, $8.314 \text{ J}.\text{K}^{-1}.\text{mol}^{-1}$

T is the temperature, in K

Comprehensive reviews of the relevant work and the associated parameter estimate variation (i.e. n spanning 1-3 and k spanning many orders of magnitude) can be found in the public literature (Duncan, 1995 and Barnes, 1999). The noted variation may arise for several reasons.

Obtaining the true value or correlation for $[\text{SiO}_2]^*$ is one such reason. There are two approaches generally used: (i) use the $[\text{SiO}_2]$ value at a large value for time (to crudely approximate $t \rightarrow \infty$). (ii) Use a solubility equation (either first reported with the kinetic work, or borrowed from other literature).

Modelling DSP precipitation rates using desilication in bauxite (Oku, 1977) is difficult – because the DSP precipitation rate cannot be divorced from the impacts of reactive silica (Re. SiO_2) dissolution so that even when the $[\text{SiO}_2]$ in liquor is decreasing with time, there will still be some Re. SiO_2 dissolving and confusing the desupersaturation rate that would occur for DSP precipitation alone.

Another possible reason for the literature variation in kinetic constants is that the conditions examined may reflect different dominating precipitation mechanisms, since not all authors have focussed on the same 'type' of desilication. The range considered has included: heater scaling (O'Neill, 1986 and Addai-Mensah, 1992), spent liquor (Thorn, 1989 and Barnes, 1999), pre-digestion (Raghavan, 1998), digestion (Tizon, 2004) and green liquor (Cresswell, 1984), with different temperatures, seed loadings and supersaturations associated with them. While it would be ideal

for one equation to encompass all the conditions, it appears probable, given the variation noted in the literature, that different mechanisms dominate different conditions.

Barnes et al (1999) identified their precipitation mechanism by comparing the products' volume based - particle size distribution (PSD) with the seed material, finding that no secondary nuclei had formed and that the increase in size suggested a growth mechanism. The authors also provide SEM images of their seed as well as their product, yet none of the images look like the characteristic wool ball structure that other literature suggests DSP to have (Ho, 1992). The fact that the fines ($<1 \mu\text{m}$) were separated in their precipitation experiments may make them less applicable to a refinery. This separation of the fines may also be the reason that the authors were able to obtain valid specific surface area (SSA) measurements at each time point for their dried out solids.

Jones and Smith (2008) focussed on the differences found in the public literature regarding kinetic constants - finding n values of 2 and 3 with k values spanning an order of magnitude. The amount of variability suggested possibly more than one precipitation mechanism. Their seed and product PSDs show product peaks at 1 and $100 \mu\text{m}$ (compared to the seed peak at $\approx 5 \mu\text{m}$), suggesting that nucleation, growth and agglomeration/aggregation were occurring simultaneously in their work.

The idea that the precipitation mechanism is not solely growth is not unheard of in the public literature. Indeed, Cousineau and Fulford (1987) noted that, at higher supersaturation, the PSD seemed to shift to smaller sizes than for lower supersaturations, where it shifted to larger sizes. Murakami et al (1992) also noted that agglomeration was occurring in seed recyclability tests. When attempting to reconcile the change in diameter of their DSP based on growth, the errors were significantly higher at lower seed loading, suggesting agglomeration was occurring.

Given the possible differences in precipitation mechanism, the work described herein sets out to identify the dominant mechanisms in DSP precipitation - initially for wide ranging conditions, but later focussing on the conditions found in pre digestion desilication tanks. Some variants of conventional methods for kinetic analysis were utilised, in the hope of obtaining relevant kinetic equations. Further experiments targeting the conditions of interest validated the empirical model framework. This was used to formulate a refinery specific pre digestion desilication kinetic equation, which was calibrated through sampling and analysis of relevant process liquors and solids.

2. Methods

2.1 Experimental Methods

Synthetic DSP was synthesised in two batches by adding kaolin ($\text{Al}_2\text{O}_3 \cdot 2\text{SiO}_2 \cdot 2\text{H}_2\text{O}$) (mine site/sigma Aldrich reagent grade) to a stirred synthetic liquor (300 g.L^{-1} NaOH (as Na_2CO_3), $\text{Na}_2\text{SO}_4 = \text{NaCl} = 10 \text{ g.L}^{-1}$) at 95°C for 24 hours. At completion, the solids were filtered and dried overnight at 60°C . The only difference in how the two batches were made up was in kaolin charge. The first batch was charged at 10 g.L^{-1} , while the second was charged at 100 g.L^{-1} . The DSP produced from the high kaolin charge was somewhat finer based on SEM imaging, which has been noted in the literature (Davis, 2010). Both products were confirmed to be sodalite/noselite-DSP ($3\text{Na}_2\text{O} \cdot 3\text{Al}_2\text{O}_3 \cdot 6\text{SiO}_2 \cdot \text{Na}_2\text{X} \cdot x\text{H}_2\text{O}$ (with $\text{X} = 2\text{Cl}, \text{SO}_4$; $x = 6-9$) with negligible kaolin, via XRD

Synthetic spent liquors were prepared and heated to 95°C in a 3 L reactor. The liquors were agitated at 300 rpm and spiked with silica (via sodium silicate, Na_2SiO_3) and then dry synthetic seed, when the reactor had reached temperature. Kinetic liquor samples were taken and filtered through a 0.45 micron filter, then analysed by titration for alumina (A), Total Caustic (as Na_2CO_3 , TC) and Total Alkali (as Na_2CO_3 , TA); and ICP-AES for Si. The experimental conditions investigated are shown in Table 1.

Based on results in the 3 L reactor experiments, a narrower range of experiments was chosen for the waterbath, to investigate the lower seed loadings and lower supersaturations in more detail.

The waterbath experiments provided kinetic solids information. In this way, an experiment at one condition involved x bottles (where x represents the number of time points, not including zero). These bottles had pre-weighed amounts of DSP seed added to them before prepared liquor was added to these heated bottles, just before they were inserted into the bottle roller and the experiment commenced. At each time point, a bottle was removed and quenched with cold water (on the outside of the bottle) before centrifuging for approximately 1 minute, so that a supernatant liquor sample could be removed for liquor analysis (ICP-AES and Titration). To prepare the solid sample, the supernatant was removed and replaced with cold 1.6 g.L^{-1} caustic to further stabilise the DSP and prevent subsequent precipitation over longer time periods. In this way, the solid samples could be analysed for PSD and by optical microscope to understand more about the mechanisms of DSP precipitation.

Table 1 – Experimental conditions

Experiment Vessel	Temperature	Seed	Supersaturation
3 L Reactor	95°C	1 (Seed 1), 10 and 100 g.L^{-1} (Seed 2)	5, 10 and 30σ
Rotating Waterbath	95°C	1, 2 and 3 g.L^{-1} (Seed 2)	3, 5 and 7σ

The only way that the solids can be adequately studied is in solution, as drying aggregates the particles and destroys the PSD.

An Accusizer (Particle Sizing Systems 770) was selected as the PSD analysis tool, as it gives a particle number distribution, rather than a volume distribution. This is an advantage when dealing with smaller particles and trying to see nucleation effects, as it is possible to have a significant number of nucleated particles that don't contribute as much to the total volume as a very few larger particles.

Lastly, a refinery specific desilication model was formulated from the data obtained sampling and analysing the relevant process streams over 2 plant surveys. Spent liquor, ex mills, desilication and blow off streams were sampled. The liquors were analysed by titration (for Alumina, A, Total Caustic, TC and Total Alkali, TA) and ICP-AES (for SiO_2), and the solids were analysed for g.L^{-1} , available alumina (Av. Al_2O_3), reactive silica (Re. SiO_2) and desilication

product silica (DSP SiO_2). Utilising the relevant process flows, a silica mass balance around the pre-digestion circuit was constructed and the DSP precipitation rate calculated for each tank. A refinery specific precipitation order and rate constant were then estimated from an appropriate $\ln(\text{solids normalised rate})$ vs. $\ln(\sigma)$ straight line fit.

2.2 Data Analysis

Lab experiment desupersaturation rates were approximated using three differences methods: forward differences, central differences and an interpolating quadratic over three points. Details are given in the appendix (A.1). k and n values were then estimated by fitting straight lines to $\ln(\text{solids normalised rate})$ vs. $\ln(\sigma)$ plots.

To determine the relative supersaturation term, σ , two solubility correlations were used: that of Hewett & White (1987) and that developed by Jamialahmadi & Muller-Steinhagen (1998).

Another kinetic parameter estimation method was also tried, whereby values for $k \times \text{SSA}$ and n were simultaneously estimated using an integral method, with the details given in the appendix (A.2).

In another approach, the desupersaturation rate equation was assumed to be: 1st, 2nd and 3rd order separately, and the area term expressed as the Specific Surface Area (SSA) multiplied by the grams per litre solids (g.L^{-1}). Rearranging the kinetic equation and evaluating the resultant integrals then provided predictions for how the SSA term must have changed with time for the order in question to be true. These predictions were compared with the observed trends in solids PSD data and microscopic imaging, as a way of checking for a realistic order value. The mathematical methods utilised to arrive at the governing SSA equations are detailed in the appendix (A.3).

The key flaw with all of the above methods is that they do not accommodate multiple mechanisms occurring concurrently.

3. Results and Discussion

There was a clear lack of consistency in the n and $k \times \text{SSA}$ values calculated, irrespective of the solubility model and numerical method. An example of this scatter is presented in Figure 1, which highlights $k \times \text{SSA}$ values generated from desupersaturation rate approximations using forward differences and an interpolating quadratic to obtain $\ln(\text{solids normalised rate})$ vs. $\ln(\sigma)$ plots, as well as those from the integral method.

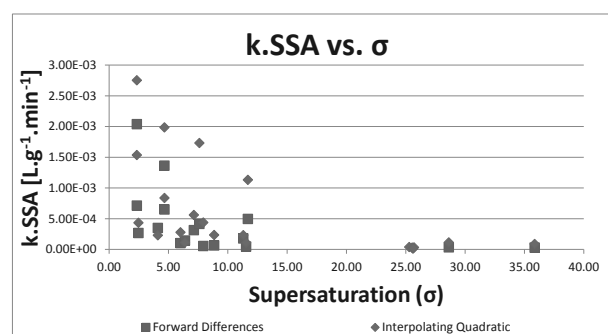


Figure 1 – Variations in estimated $k \times \text{SSA}$ values with supersaturation, σ , (calculated using the Hewett & White (1987) solubility equation), using data from all reactor and waterbath experiments with seed 2. Similar scatter was noted for Jamialahmadi (1998) solubility.

It was expected there should have been greater consistency if a single precipitation mechanism had dominated all the reactor and water bath experiments. As shown by Figure 2, the product PSDs from the 3 L reactor experiments clearly show more than one mechanism at play – with more nucleation at higher seed

loadings and a greater amount of agglomeration and possibly growth occurring in the lower seed loadings. Note that the 1 g.L⁻¹ experiment is generated from Seed 1, and the 100 g.L⁻¹ experiment is from Seed 2.

Collection of kinetic solids information for the experiments at lower supersaturations and seed loadings further suggests that an agglomeration event took place in the very early stages of the experiments. The PSDs, together with the optical microscopy images in Figure 3, show this effect. The higher magnification images, for example Figure 4, show the larger particles to be made of discrete smaller particles, further suggesting aggregation. To very roughly describe the precipitation mode – upon contacting the supersaturated liquor, the DSP seed appears to have immediately agglomerated and then started to concurrently nucleate and further agglomerate.

None of the SSA time trends back calculated from 1st, 2nd or 3rd order kinetic equations (using the method detailed in Appendix A.2) agreed with the observed SSA trends. All orders tested suggested an increase in SSA through time (to different degrees) as opposed to the decrease observed. The difference exists because none of the kinetic equations examined account for precipitation with agglomeration.

Subsequent testing was done to ensure that the observed agglomeration was real as well as realistic for a pre digestion setting. The first further test was to investigate whether agglomeration was a by-product of the experimental conditions rather than the actual supersaturation. To explore this, the same liquor was used but without silica added (under saturated). The liquor was combined with seed and left in the waterbath for 60 minutes. As the liquor was below DSP solubility, the DSP dissolved, which of course meant that the number of fines decreased due to the dissolution. However, this decrease was not enough to suggest agglomeration was also occurring. Nor was there a noticeable shift to a coarser PSD, as would have occurred with agglomeration. The apparent absence of agglomeration in this test is corroborated by the optical microscopy images in Figure 5.

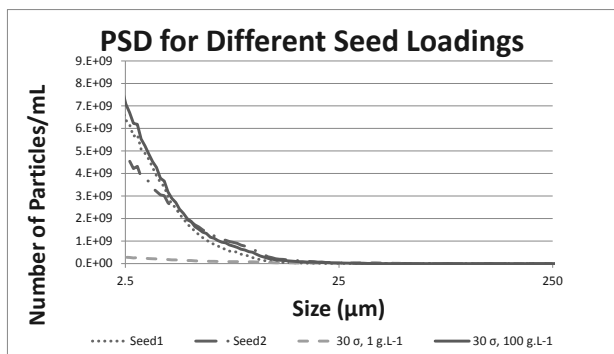


Figure 2 – Resultant PSDs for different seed loading at the completion of the experiment, showing both agglomeration and nucleation for different conditions. Seed 1 produced the 1 g.L⁻¹ solids, Seed 2 produced the 100 g.L⁻¹ solids

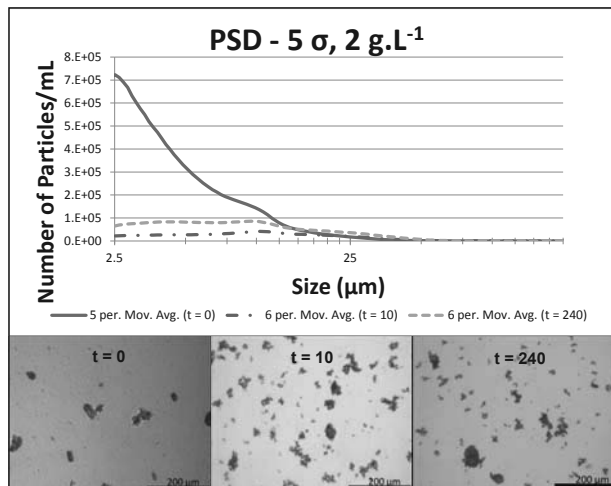


Figure 3 – PSD evolution through time with accompanying microscopy images.

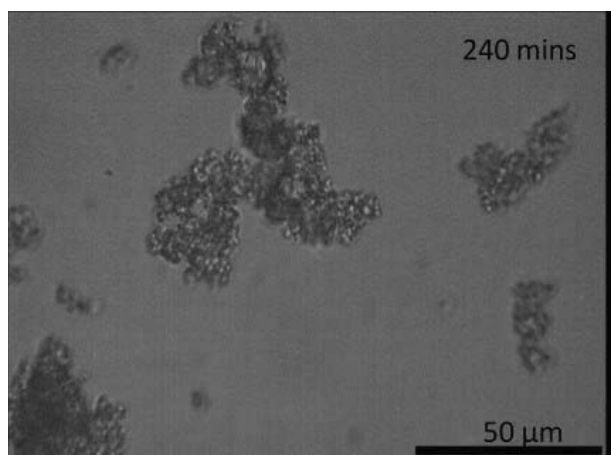


Figure 4 – 5 σ, 2 g.L⁻¹ DSP at 240 minutes – higher magnification showing discrete particles that make up aggregates.

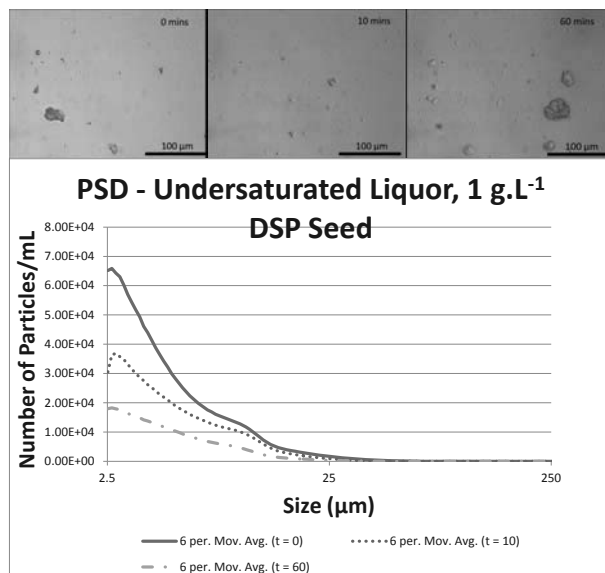


Figure 5 – PSDs and optical images for under saturated liquor highlighting no agglomeration without supersaturation. The decrease in particle number is attributed to DSP dissolution (i.e. <math>< \sigma</math>) and not agglomeration because the PSD peaks do not shift.

It was logically thought that the possibility of agglomeration under pre digestion conditions (i.e. $\approx 1000 \text{ g.L}^{-1}$ solid loading) would be quite low. Perhaps the DSP particles could agglomerate in the system tested because of the greater freedom for like particle collisions. To test this, a supersaturated liquor was mixed with 5 g.L^{-1} DSP seed but also with other non-DSP solids. These tests were also used to check whether the other solid surfaces could act as nucleation sites for DSP precipitation. Six bottles were tested simultaneously, and the results are shown below in Figure 6. These results suggest that DSP can secondarily nucleate off any surface – the greater the surface area, the greater the impact.

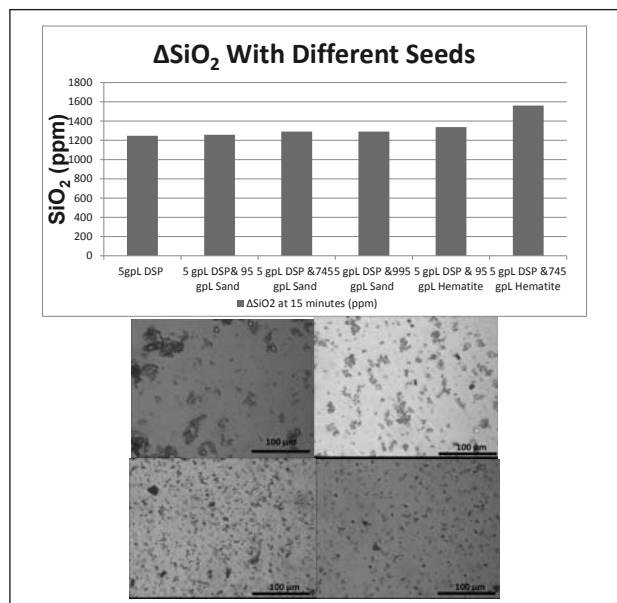


Figure 6 – SiO_2 desupersaturation and microscopy images showing secondary nucleation increasing with solids concentration. Optical images: Top Left: 5 g.L^{-1} DSP; Top right: 5 g.L^{-1} DSP & 95 g.L^{-1} Sand; Bottom Left: 5 g.L^{-1} DSP & 745 g.L^{-1} sand; Bottom right: 5 g.L^{-1} DSP & 995 g.L^{-1} sand.

Imaging was also possible for the DSP from the DSP + sand samples because the coarse sand readily settled out leaving the fines in the supernatant, and is also shown in Figure 6. Of course it is possible that larger DSP particles also settled in with the sand, or became occluded with them, so the images are not absolute confirmation of the precipitation mode. It appears that the greater the sand loading, the finer and more plentiful the solids are in the supernatant.

Having realised that secondary nucleation is likely to be the dominant precipitation mechanism for a pre-digestion high solids desilication circuit, a traditional kinetic analysis was applied to process data, using the DSP SiO_2 solids concentrations from plant circuit survey data.

To accommodate the increasing concentration of DSP solids throughout the desilication circuit, the rate (as determined by backward DSP mass flow differences) was standardised with the DSP solids concentration (in grams per litre) before correlating the logarithms of these standardised rates with the logarithms of the relevant super saturation terms. i.e.:

$$\begin{aligned} d[\text{SiO}_2]/dt &= k.(\text{SSA}).(\text{DSP solids g.L}^{-1}).\sigma^n \\ d[\text{SiO}_2]/dt / (\text{DSP solids g.L}^{-1}) &= k.\text{SSA}.\sigma^n \\ \ln [d[\text{SiO}_2]/dt / (\text{DSP solids g.L}^{-1})] &= \ln(k.\text{SSA}) + n.\ln(\sigma) \end{aligned}$$

where

$$\begin{aligned} k &= k_0.e^{(-E_a/RT)}, \text{ in } \text{g.m}^{-2}.\text{h}^{-1} \\ d[\text{SiO}_2]/dt &\text{ is the DSP production rate (g.L}^{-1}.\text{h}^{-1}) \end{aligned}$$

Surveys were conducted over two days and the resulting kinetic correlation is given in Figure 7. The circuit investigated had two parallel series (of 3 and 4 tanks respectively), so effectively 4 desilication processes were investigated. Statistical analysis of the correlated data yielded an order of $n = 1.81 \pm 0.63$. Therefore, the refinery specific pre-digestion DSP precipitation kinetic equation is:

$$d[\text{SiO}_2]/dt = k.(\text{DSP solids g.L}^{-1}).\sigma^{(1.81 \pm 0.63)}$$

Activation energy and temperature effects were ignored as the circuit runs at a relatively constant temperature, close to 95°C . It is difficult to compare the estimated rate constant to the literature as it still needs to be standardised by an Arrhenius term, involving estimation of the relevant activation energy, E_a , and a DSP SSA term (potentially unique to this circuit). To obtain a true k_0 , further work will be required under nucleation conditions at varying temperatures, to estimate the relevant pre-digestion activation energy. To obtain an absolute k_0 , potentially transferable between pre digestion desilication circuits, adequate measures of DSP SSA would also be required. The estimated order, $n \approx 2$, is in agreement with that most frequently reported in the literature.

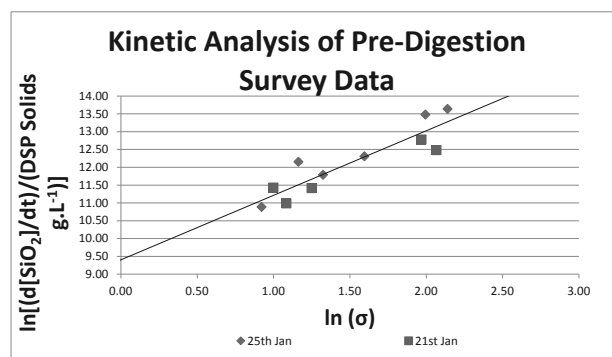


Figure 7 – Kinetic analysis yielding order and rate constant for a refinery pre-digestion circuit.

4. Conclusions

This work has shown that DSP precipitation is not governed by one mechanism in isolation. While agglomeration was shown as a real event in the laboratory experiments, further work replicating pre-digestion, high solids desilication conditions has shown secondary nucleation to be dominant. Together with refinery sampling, this information has enabled a refinery specific, empirical pre-digestion desilication kinetic equation to be developed (but not readily be extended to other types of desilication processes). This work has shown that much of the disparity in the literature may in fact be an artefact of different precipitation mechanisms for different experimental conditions.

5. Acknowledgements

Alcoa World Alumina's TDG Analytical Services Group for solids and liquor analyses. Mr. Mark Jones for assistance with plant surveys. Mr. Shannon Dye, Dr. Mitch Loan and Dr. Geoff Riley for providing direction, general discussions and proof reading.

6. Appendix

A.1. The Difference Methods

- (i) Forward Differences: $(d\sigma/dt)_t = (\sigma_{t+dt} - \sigma_t)/dt$
 (ii) Central Differences: $(d\sigma/dt)_t = (\sigma_{t+dt} - \sigma_{t-dt})/2dt$
 (iii) Interpolating Quadratic = $(d\sigma/dt)_t = a + 2b(t-t_1)$
 $a = [(\sigma_2 - \sigma_1)/(t_2 - t_1)^2 - (\sigma_3 - \sigma_1)/(t_3 - t_1)^2] / [1/(t_2 - t_1) - 1/(t_3 - t_1)]$
 $b = [(\sigma_2 - \sigma_1)/(t_2 - t_1) - (\sigma_3 - \sigma_1)/(t_3 - t_1)] / (t_2 - t_3)$

For (iii), 3 points are supplied – (t_1, σ_1) ; (t_2, σ_2) ; (t_3, σ_3) ; and t is in the range $[t_1, t_3]$

A.2. The Integral Method

$$-d\sigma/dt = k.A.\sigma^n$$

$$-\sigma^n . d\sigma/dt = k.A$$

$$d(\sigma^{n+1}/(n+1))/dt = k.A$$

$$1/(n+1) \cdot ((1/\sigma_t^{n+1}) - (1/\sigma_0^{n+1})) = k.A.t \quad (\text{by integration, assuming A essentially constant through time})$$

$$(1/\sigma_t^{n+1}) - (1/\sigma_0^{n+1}) = k.A.t.(n+1)$$

$$(\sigma_0^{n+1}/\sigma_t^{n+1}) = 1 + k.A.t.(n+1) \cdot \sigma_0^{n-1} \quad (\text{by multiplying by } \sigma_0^{n-1} \text{ and rearranging})$$

$$\sigma_t = \sigma_0 / [1 + k.A.t.(n+1) \cdot \sigma_0^{n-1}]^{1/(n-1)} \quad (\text{by rearranging again and raising both sides to the } 1/(n-1)^{\text{th}} \text{ power})$$

Thus, using actual σ_t measurements for each time point, k and n can be estimated (under constant A , constant mechanism assumptions) by minimising residual sums of squares.

A.3. SSA Tracking

Assume the order is 2 (for example) then express the area term, A , as the specific surface area multiplied by the grams per litre solid DSP, before then expressing the $g.L^{-1}$ DSP in terms of the change in the dissolved $[SiO_2]$ concentration and S = the initial $g.L^{-1}$ solid seed:

$$-d\sigma/dt = k.(SSA).(g.L^{-1} DSP).\sigma^2$$

$$-d\sigma/dt = k.(SSA).(S + \sigma_i.[SiO_2]^* - \sigma_i.[SiO_2]^*).\sigma^2$$

$$\int -d\sigma/(S + \sigma_i.[SiO_2]^* - \sigma_i.[SiO_2]^*).\sigma^2 = k. \int SSA(t).dt$$

The left hand side is an integral of the form:

$$\int -dx/[(a-kx).x^2]$$

which, by the method of partial fractions, has the following solution:

$$\{k.x.[\ln(a-kx) - \ln(x)] + a\}/a^2.x$$

Substituting the values for k and a , as well as substituting σ for x gives:

$$\{[SiO_2]^*.\sigma_i.[\ln(S + \sigma_i.[SiO_2]^* - \sigma_i.[SiO_2]^*.\sigma) - \ln(\sigma_i)] + S + \sigma_i.[SiO_2]^*\}/[(S + \sigma_i.[SiO_2]^*)^2.\sigma_i] = k. \int_0^t SSA(t).dt$$

So a plot of the left hand side versus time should yield the integral of the specific surface area multiplied by k . The derivative of this function with respect to time (numerically determined by difference methods) then gives a plot of SSA vs. t .

References

- 1) Duncan, A, Muller-Steinhagen, H, Verity, B, Welch, B, 1995, 'An Investigation Of Desilication Kinetics In Spent Bayer Liquor', *Light Metals*, pp. 37-44.
- 2) Barnes, M, Addai-Mensah, J, Gerson, A, 1999, 'The Kinetics Of Desilication Of Synthetic Spent Bayer Liquor Seeded With Cancrinite And Cancrinite/Sodalite Mixed-Phase Crystals', *Journal Of Crystal Growth*, vol. 200, pp. 251-264.
- 3) Oku, T & Yamada, K, 1971, 'The Dissolution Rate Of Quartz And The Rate Of Desilication In The Bayer Liquor', *Light Metals*, pp. 31-45.
- 4) O'Neill G, 1986, 'Prediction of Heat Exchanger – Heat Transfer Coefficient Decay Due To Fouling', *Light Metals*, pp. 133-140.
- 5) Addai-Mensah, J, Gerson, A, Zheng, K, O'Dea, A, Smart, R, 1997, 'The Precipitation Mechanism Of Sodium Aluminosilicate Scale In Bayer Plants', *Light Metals*, pp.23-28.
- 6) Thorn, S & White, A, 1989, 'Desilication Kinetics Of Spent Liquor', *Alcoa Internal Report*.
- 7) Raghavan, N & Fulford, G, 1998, 'Mathematical Modeling Of The Kinetics of Gibbs Extraction And Kaolinite Dissolution', *Light Metals*, pp. 29-37.
- 7) *Alcoa Internal Report*.
- 8) Tizon, E, Clerin, P, Cristol, B, 2004, 'Effect of Predesilication And Digestion Conditions On Silica Level In Bayer Liquor', *Light Metals*, pp. 9-15.
- 9) Cresswell, P, 1984, 'Factors Affecting Desilication Of Bayer Process Liquors', *Chemeca 84*, pp. 285-292.
- 10) Barnes, M, Addai-Mensah, J, Gerson, A, 1999, 'The Kinetics Of Desilication Of Synthetic Spent Bayer Liquor And Sodalite Crystal Growth', *Colloids and Surfaces A: Physicochemical and Engineering Aspects*, vol. 147, pp. 283-295.
- 11) Ho, G, Robertson, W, Roach, G, Antonovsky, A, 1992, 'A Morphological Study Of Bayer Process Desilication Product And Its Application to Laboratory And Plant Digests', *Industrial Engineering Chemical Research*, vol. 31, pp. 982-986.
- 12) Jones, F & Smith, P, 2008, 'What Is The Kinetic Order Of Desilication?', *Proceedings Of The 8th International Alumina Quality Workshop*, pp. 100-102.
- 13) Cousineau, P, Fulford, G, 1987, 'Aspects Of The Desilication Of Bayer Liquors', *Light Metals*, pp. 11-17.
- 14) Murakami, M, Ishibashi, K, Kumagai, Y, Harato, T, 1992, 'Aspect Of Desilication Kinetics With Recycled Seed', *Light Metals*, pp. 13-16.
- 15) Davis, M, Dai, Q, Chen, WH, Taylor, M, 2010, 'New Polymers For Improved Flocculation Of High DSP-Containing Muds', *Light Metals*, pp. 57-61.
- 16) *Alcoa Internal Report*.
- 17) Jamialahmadi, M, Muller-Steinhagen, H, 1998, 'Determining Silica Solubility In Bayer Process Liquor', *Journal Of Metals*, pp. 44-49.